Colloid Polym Sci (2004) 282: 429–439
DOI 10.1007/s00396-003-0963-5

ORIGINAL CONTRIBUTION

N. Grozev
V. Aguié-Béghin
B. Cathala
R. Douillard
I. Panaiotov

Kinetics and layer organization during the polymerization of coniferyl alcohol at the air-water interface

Received: 18 November 2002
Accepted: 9 July 2003
Published online: 14 October 2003

N. Grozev · I. Panaiotov (✉)
Biophysical Chemistry Laboratory,
University of Sofia, J. Bourchier 1 str.,
1126 Sofia, Bulgaria
E-mail: ipanaiotov@chem.uni-sofia.bg

V. Aguié-Béghin · B. Cathala
R. Douillard
Unité Mixte de Recherche
"Fractionnement des Agro-Ressources et Emballage", INRA,
CRA, 2 Espl. R. Garros, BP224,
51686 Reims Cedex 2, France

Abstract The initial stage of the polymerization of coniferyl alcohol catalyzed by a peroxydase was studied at the air-water interface. The properties of the monolayers were investigated at constant area and at constant surface pressure by surface pressure, surface potential and ellipticity measurements. On the basis of the results obtained at constant surface area, it is proposed that the formation of a 2D layer occurs up to the inflection point of the surface pressure-area isotherm, and that for larger surface pressures a 3D structure is formed during the polymerization. If the barostat is set at the inflection point (the surface pressure is constant while the surface area increases), the 2D organization of the monolayer is retained. A kinetic model describing the adsorption of the reaction products in a 2D layer is proposed. The kinetic constants were determined from the surface potential, ellipsometry, surface pressure and surface area data.

Keywords Monolayers · Coniferyl alcohol · Horseradish peroxidase · Ellipsometry

Introduction

Lignin is a complex natural macromolecule, which participates in the construction of the plant cell wall, along with cellulose and hemicelluloses. It is constituted mainly of three phenyl-propane units (guaiacyl, syringyl and p-hydroxyphenyl). These structural elements are linked through 11 different types of covalent bonds [1, 2, 3], forming a three-dimensional network which contributes to the resistance of the plant cell to mechanical, chemical or biological stresses. Despite the small number of monomers, the structure of native lignin is still not resolved. The biosynthesis of lignin is accomplished with the participation of cell wall peroxidases. They mediate, in the presence of H_2O_2, the formation of radicals from the phenyl-propane species (see Fig. 1).

Dehydrogenation polymers (DHPs) can be used as model compounds of lignins [4]. The synthesis of these polymers is studied mainly in bulk conditions and is found to be very reproducible and free from sugar contamination [5]. Nowadays there is increasing interest in studying the properties of lignin and DHPs spread as monolayers at the air-water interface [6, 7, 8]. The reason for this is that this system can mimic the hydrophilic-hydrophobic interface in the plant cell wall (lignin-hemicellulose). In a previous paper [9] the physicochemical properties of monolayers of lignins and of two DHP-polyguaiacyl (DHPG) and poly(guaicyl-co-siringyl) (DHPGS), were compared. The most important conclusion was that the molecular organization of the adsorption layers is a function of the spread quantity. The layers exhibit a mostly two-dimensional organization for low spread amounts and this organization is expected to be more or less three dimensional for highly deposited quantities.

The effect of an interface on the mechanism and on the kinetics of polymerization until recently received little attention. The air-water interface can be used as a model for the reactions proceeding in the plant cell wall

during lignification. To our knowledge only a few papers have been dedicated to this kind of study [10, 11, 12, 13]. In one previous paper [13] the process of polymerization at the air-water interface with 0.0375 mg.m^{-2} spread horseradish peroxidase (HRP) and 10 mg.L^{-1} coniferyl alcohol (CA) in water was monitored by surface pressure, ellipticity and neutron reflectivity measurements.

In this paper we present results obtained at the beginning of the interfacial polymerization with different spread quantities of enzyme and concentrations of substrate (CA) performed in two distinct conditions: at constant area, A = const (the surface pressure is increases); and at constant surface pressure, π = const (the area, occupied by the interfacial layer increases with time). The course of the initial stage of the peroxydase mediated polymerization of coniferyl alcohol and the properties of the consequently formed monolayers at the air-water interface were investigated by surface pressure, surface potential and ellipsometry. We also propose a kinetic model for the interfacial polymerization.

Experimental

Materials

Coniferyl alcohol (CA) was synthesized as previously described [14] and was used in a solution of phosphate buffer (1/30 N, pH 5.5). The CA concentrations were 5, 6, 6.5, 7, 10, 15 and 20 mg.L^{-1}.

Peroxidase solution 2.13 mg of Peroxidase type VI (Sigma, 250–330 units.mg^{-1}) was dissolved in 20 ml of the same phosphate buffer. The spread quantities, Γ_E, were 0.2, 0.15, 0.1, 0.075 and 0.05 mg.m^{-2} using the Trurnit method [15] and a total volume of solution of 18 μL on an area of 91.56 cm^2. The glass rod was carefully cleaned and put in vertical position.

Hydrogen peroxide solution (30% w/w in water, Sigma, Germany) was deposited as little drops at the air-water interface. The deposited amount was 130 μL H_2O_2 solution for 100 mL subphase.

Measurements at the air—water interface

The dependence of the enzymatic polymerization on the order and the method used to spread the reagents was investigated. The tested procedures were:

1. Spreading of the enzyme at the air-solution interface by droplet deposition. After a period of 5 min the hydrogen peroxide solution was spread by the same procedure.
2. Spreading of hydrogen peroxide solution, followed by droplet deposition of the enzyme.
3. Spreading of hydrogen peroxide solution and then spreading of the enzyme by the Trurnit method. The glass rod used was in the vertical position.

From the above experiments it was found that the third method gives the best results (greatest change in surface pressure and in ellipticity as well as the best reproducibility). It was used throughout this work.

It is worth mentioning that at the end of the experiments there was some material adsorbed on the platinum Wilhelmy plate. The latter was carefully cleaned using consequent soaking in dioxan, ethanol, and RBS, and finally flamed.

For all spread amounts of HRP no interfacial protein layer was detected by tensiometry or by ellipsometry.

The surface pressure (π) was measured using a KSV-2200 (Finland) or KSV minitrough surface balance equipped with a platinum Wilhelmy plate. The surface potential (ΔV) was measured simultaneously using a gold-coated ^{241}Am ionizing electrode, a reference electrode and a KP 511 (Kriona, Bulgaria) electrometer, connected to a PC with user software for real-time data measurements. As usual, the surface potential of the pure aqueous surface fluctuated for about 30 minutes. When the air-water surface potential became constant, spreading of the monolayer could be performed. The accuracy of the initial surface potential value was $\pm$15 mV.

Four experiments were performed:

1. The polymerization was monitored at constant area for all mentioned enzyme and substrate concentrations via surface pressure π(t) and surface potential $\Delta V(t)$ measurements.
2. The increase of the surface area $\Delta A(t)$ and the evolution of $\Delta V(t)$ during the polymerization reaction at constant surface pressure (π_i = 1 mN.m^{-1}) were measured for 20 mg.L^{-1} and 10 mg.L^{-1} concentrations of coniferyl alcohol, and for 0.2 mg.m^{-2} and 0.1 mg.m^{-2} spread enzyme.
3. Surface rheology experiments were performed by measuring the surface pressure variations at several distances x_i, as a function of time during and after a small compression ($\Delta\pi$ = 0.5 mN.m^{-1}) of the monolayer. The system contained 6.5 mg.L^{-1} coniferyl alcohol (C_{CA} = 6.5 mg.L^{-1}) and 0.2 mg.m^{-2} spread enzyme. The rheological measurements were performed after 2 hours of polymerization when the surface pressure was stabilized. The compressions were performed with two velocities U_b = 180 cm^2 min^{-1} and U_b = 10 cm^2 min^{-1} for each distance x_i. As a result of the surface density gradient, caused by the continuous local surface pressure perturbation, a simultaneous motion of the monolayer and of the liquid substrate occurred (the so-called Marangoni effect) with characteristic time of propagation τ_M. The surface motion is practically dilatational and can be detected by measuring the change of the surface pressure $\Delta\pi$. It is appropriate to analyze separately the cases of relaxation processes with characteristic times θ of the order of magnitude of τ_M, and that of τ, many orders of magnitude larger than τ_M. In the first case ($\theta \approx \tau_M$) the relaxation processes accompany the Marangoni propagation process along x and a fan-like dependence of the slopes $\left(\frac{d\Delta\pi}{dt}\right)$ on the distance x is

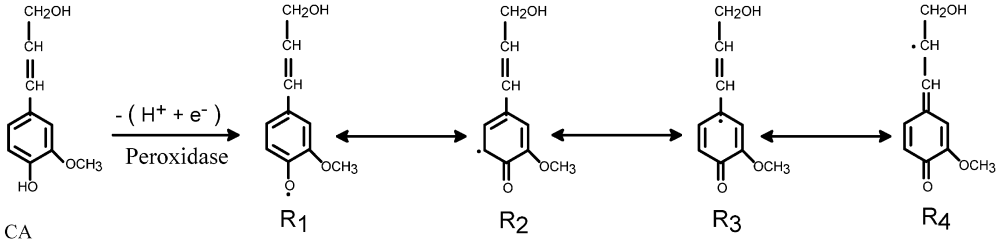

Fig. 1 Formation of mesomeric stabilized radicals (R_i) from coniferyl alcohol (CA) catalyzed by the enzyme Horseradish Peroxidase

observed. The following expression for the slope in the quasi-steady region of the compression is obtained [16, 17]:

$$\frac{d\Delta\pi}{dt} = E_d U_b \alpha \frac{ch\alpha(L_0 - x)}{sh\alpha L_0}$$

where $\alpha^{-1} = \sqrt{D_u\theta}$ is the characteristic length of propagation along a Maxwell viscoelastic monolayer spread on a liquid viscous subphase. In the second case ($\tau >> \tau_M$), the re-equilibration time of the surface pressure gradient along x is much smaller than τ (the characteristic time of the surface relaxation process) and the dynamic response of the monolayer can be considered as a whole, neglecting the Marangoni effect. In order to describe the surface pressure change ($\Delta\pi = \pi(t) - \pi_{ini}$) during the compression c of duration T with a constant velocity U_b followed by a relaxation r at constant area, it is assumed that at any time, the total surface pressure change $\Delta\pi = \pi(t) - \pi_{ini}$ can be represented by the sum of equilibrium $\Delta\pi_e$ and a non-equilibrium $\Delta\pi_{ne}$ contributions: $\Delta\pi = \Delta\pi_e + \Delta\pi_{ne}$

The equilibrium part $\Delta\pi_e$ is related to the equilibrium surface dilatational elasticity E_e, while the non-equilibrium part of the total surface pressure change $\Delta\pi_{ne}$ is associated with the accumulation of elastic energy during the compression. Dissipation of this accumulated energy through molecular mechanisms occurs during compression as well as relaxation. The analysis of this case based on the generalized Maxwell model with two characteristic times gives the following equations describing the viscoelastic behavior of the monolayer [18]:

$$\Delta\pi = E_e \frac{U_b t}{L_0} + E_{ne_1} \frac{U_b \tau_1}{L_0}\left(1 - e^{-t/\tau_1}\right) + E_{ne_2} \frac{U_b \tau_2}{L_0}\left(1 - e^{-t/\tau_2}\right) \quad (1)$$

and the relative relaxation when the time of compression T is much smaller than the time of the relaxation process ($T << \tau_1$ and τ_2)

$$\frac{\pi(t) - \pi_\infty}{\pi_0 - \pi_\infty} = \frac{E_{ne_1}}{E_{ne_1} + E_{ne_2}} e^{-t/\tau_1} + \frac{E_{ne_2}}{E_{ne_1} + E_{ne_2}} e^{-t/\tau_2} \quad (2)$$

After differentiation of Eqn. 1 with respect to time and with the simplification

$$E_{ne_1} \approx E_{ne_2} \approx \frac{E_{ne}}{2}$$

the following expression for the slope $\left(\frac{d\Delta\pi}{dt}\right)_x$ during the compression can be obtained:

$$\frac{d\Delta\pi}{dt} = E_e \frac{U_b}{L_0} + \frac{E_{ne} U_b}{2} \frac{\left(e^{-t/\tau_1} + e^{-t/\tau_2}\right)}{L_0} \quad (3)$$

It is obvious that in the quasi-steady region the slopes do not depend on the distance x.

4. Surface polymerization was investigated by means of ellipsometry. Measurements were performed using a spectroscopic phase modulated ellipsometer (UVISEL, Jobin Yvon, Longjumeau, France). It was equipped with a xenon arc lamp. In the chosen configuration, the polarizer and the analyzer were set to 45°, and the photoelastic modulator (activated at a 50 kHz frequency) was set to the 0° orientation. The measurements were monitored at the angle of incidence of 53°4. The two ellipsometric angles ψ and Δ are linked to the two reflectivity coefficients r_p and r_s in the direction parallel and perpendicular to the incidence plane respectively by:

$$\frac{r_p}{r_s} = tg\psi \exp(i\Delta) \quad (4)$$

The fixed wavelength chosen for the kinetic measurements corresponds to the Brewster conditions of the substrate defined by:

$$\Delta = \pm\frac{\pi}{2} \quad (5)$$

The ellipticity coefficient of the absorption layer in the Brewster conditions, $\overline{\rho_B}$ is defined by:

$$\overline{\rho_B} = tg\psi \sin\Delta \quad (6)$$

The ellipticity measured at this angle is very sensitive to any structure at the interface, and the magnitude of the ellipticity is indicative of the amount of adsorbed molecules [19].

In all experiments, the ellipsometric spectrum in the range 240–820 nm was determined after two hours of polymerization. The spectra were analyzed using the model of a single, homogeneous and transparent layer in the range between 415 – 800 nm. As a first approximation the Cauchy dispersion law was used:

$$n(\lambda) = A + \frac{B}{\lambda^2} + \frac{C}{\lambda^4},$$

where A, B and C are constants and λ is the wave length in nm. With this dispersion law the thickness, h, of the adsorbed layer could be estimated.

The surface concentration of the adsorbed molecules was estimated using the equation of De Feijter [20, 21]:

$$\Gamma = \frac{\left(n_{layer} - n_{substrate}\right)}{\frac{dn}{dc}} h \quad (7)$$

where n_{layer} is the refractive index in the adsorbed layer at 589 nm, $n_{substrat}$ is the refractive index of the solution at 589 nm, and $\frac{dn}{dc} = 0.173 g^{-1}cm^3$ is the refractive index increment of the solute.

All experiments were performed at temperature 20 ± 2° C.

Results and discussion

The polymerization process was simultaneously monitored by tensiometry and ellipsometry, as well as by surface potential measurements. The occurrence of coniferyl alcohol in the solution (with or without spread enzyme at the surface) did not change the surface pressure or the ellipticity of the pure buffer (data not shown), indicating that CA does not form an adsorption layer at the air interface and that the spread enzyme has no significant effect on the surface properties of the buffer. Moreover, when no HRP is added to the system, there is no change in the surface pressure, in the surface potential or in the ellipticity (data not shown), which confirms the key role of the enzyme in the interfacial polymerization.

The reaction rate during the initial stage of surface polymerization is a function of the enzyme concentration. From the experimental results presented in Fig. 2, it is obvious that an increase of the amount of spread enzyme reduces the lag time, increases the rate of surface pressure rise, and that of ellipticity decrease.

The rate of the reaction during its initial stages is also an increasing function of the CA in the subphase (see Fig. 3). The perturbation of the ellipsometric

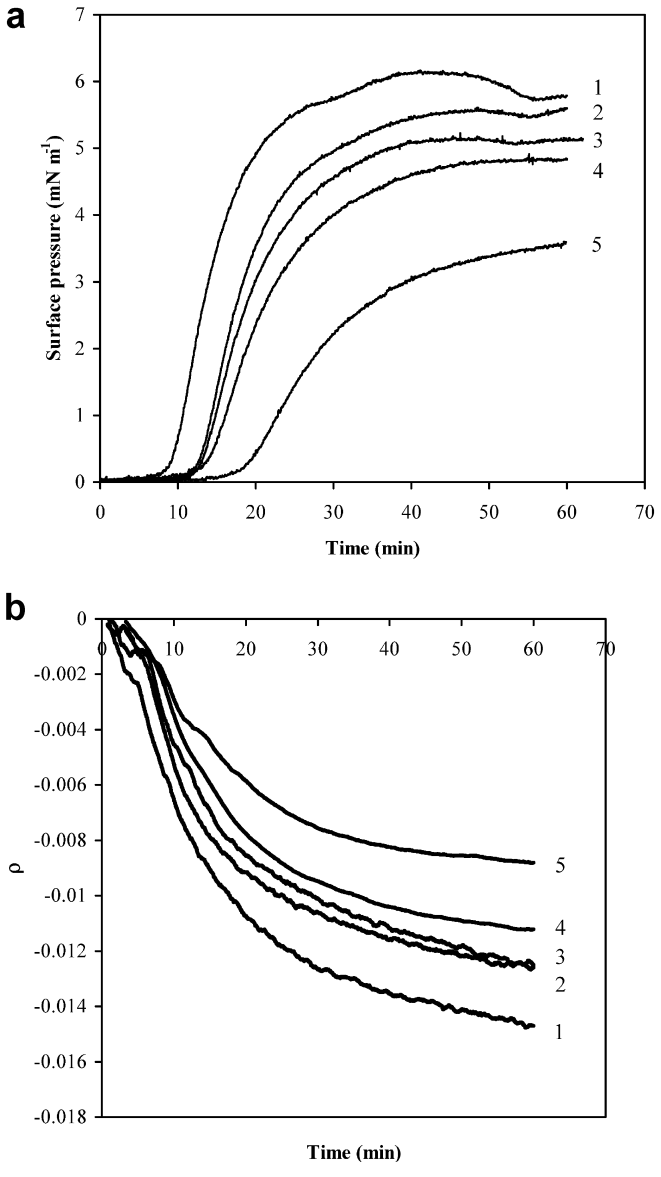

Fig. 2 Dependence of enzyme concentration on the reaction rate. The studied systems contain 10 mg.L^{-1} CA + differing quantities of HRP: 1: 0.2 mg.m^{-2}, 2: 0.15 mg.m^{-2}, 3: 0.10 mg.m^{-2}, 4: 0.075 mg.m^{-2}, 5: 0.05 mg.m^{-2}. **a** surface pressure evolution with time. **b** the decrease in ellipticity, measured simultaneously for the same experiments

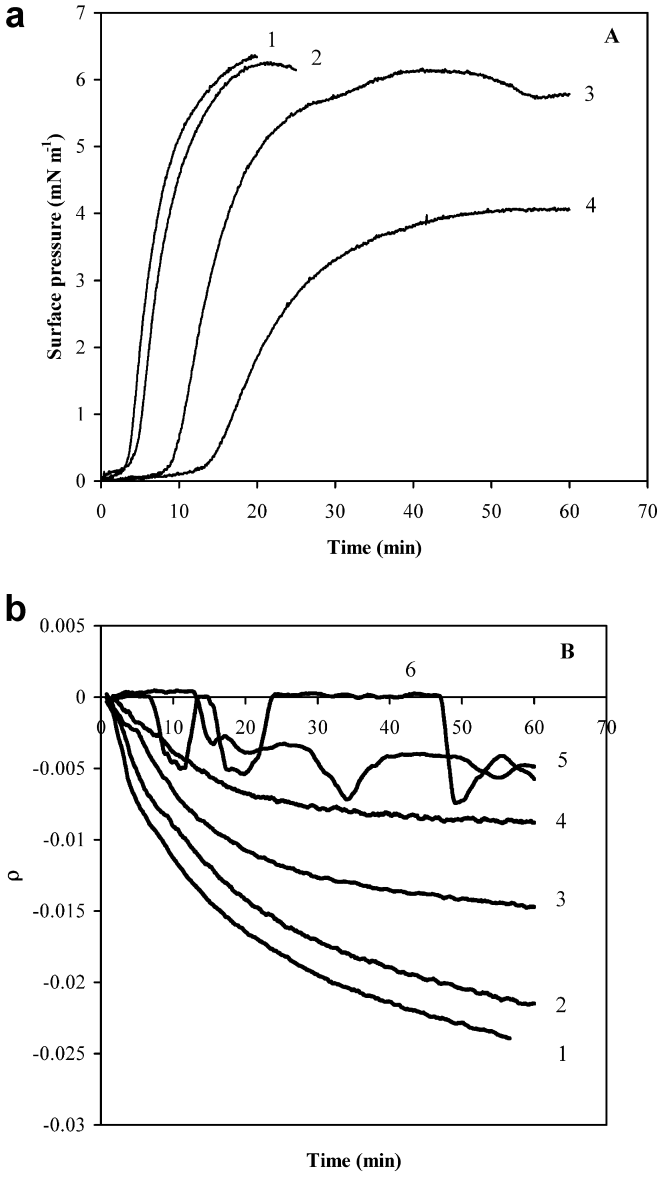

Fig. 3 Dependence of the reaction rate on the substrate (CA) concentration. The studied systems contain 0.2 mg.m^{-2} HRP + differing quantities of CA: 1: 20 mg.L^{-1}, 2: 15 mg.L^{-1}, 3: 10 mg.L^{-1}, 4: 7.5 mg.L^{-1}, 5: 6 mg.L^{-1}, 6: 5 mg.L^{-1} . **a** surface pressure evolution with time. **b** the decrease in ellipticity, measured simultaneously for the same experiments. The ellipsometric measurements detect the presence of reaction product at the surface, in contrast to tensiometry in the case of 6 mg.L^{-1} and 5 mg.L^{-1} CA

signal for curves 5 and 6 is probably due to the presence of non-connected domains at the surface. As can be seen the surface pressure method detects the course of the reaction with concentrations of CA above 6.5 mg.L^{-1}. The polymerization at CA concentrations of 5 and 6 mg.L^{-1}, could be detected only by ellipsometry. The surface thickness and surface concentration were estimated from the ellipsometric data (see Table 1). The thickness varies between 48 Å (for 7.5 mg.L^{-1}) and 53 Å (in the case of 20 mg.L^{-1}), and the surface concentration is in the range of 3 – 6 mg.m^{-2} respectively.

The presence of surface-active products of the reaction was also monitored by the evolution of the surface potential over time. The results obtained for systems of 10 mg.L^{-1} CA and concentrations of HRP equal to 0.2 mg.m^{-2} and 0.1 mg.m^{-2} at constant area are presented in Fig. 4. ΔV changes rapidly at the beginning of

Table 1 The change in the surface pressure and in the ellipticity for layers formed by the products of the interfacial polymerization of different quantities of coniferyl alcohol (CA) and 0.2 mg.m^{-2} HRP. The greater the concentration of the CA, the greater the increase of π, the decrease of $\bar{\rho}_B$ and the shorter the lag-time (τ_{lag}). From the ellipsometric spectrum data the thickness (h) and the refractive index (n_{layer}) of the interfacial layer were estimated using as a first approximation the Cauchy dispersion law: $n(\lambda) = A + \frac{B}{\lambda^2} + \frac{C}{\lambda^4}$, where A, B and C are constants and λ is the wavelength in nm. The surface concentration was estimated by use of Eqn. 7 (see main article text for more details)

CA (mg.m^{-2})	Surface pressure (π)		Ellipticity ($\bar{\rho}_B$)		Estimates		
	τ_{lag} (min)	π_{max} (mN.m^{-1})	τ_{lag} (min)	$\lvert\bar{\rho}_{B(eq)}\rvert$	h (Å)	n_{layer}	Γ (mg.m^{-2})
5.0	∞	0	~2	$0 < \lvert\bar{\rho}_B\rvert < 0.0075$	–	–	–
6.0	∞	0	~2	$0 < \lvert\bar{\rho}_B\rvert < 0.0075$	–	–	–
7.5	17.5	4.3	1.5	0.0095	48.2	1.4368	2.9
10.0	11.0	5.9	1	0.0140	44.1	1.4769	3.7
15.0	5.0	6.1	< 1	0.0210	44.1	1.5604	5.8
20.0	4.0	9.2	< 1	0.0240	53.1	1.5336	6.1

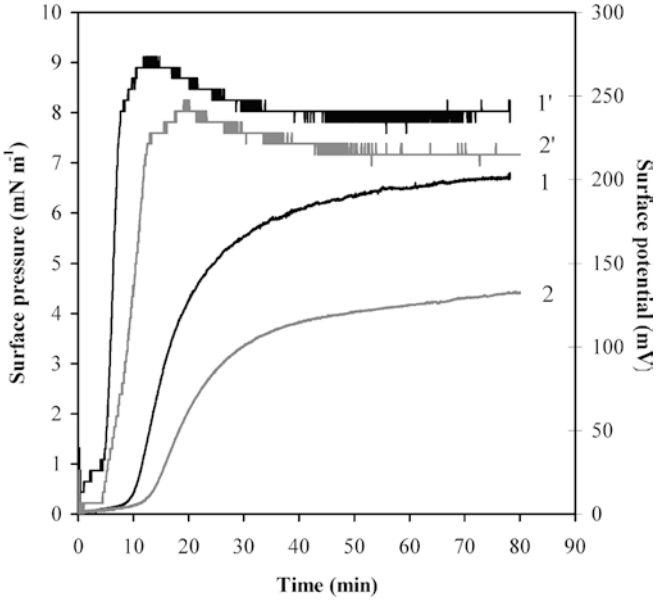

Fig. 4 Evolution of the surface pressure and the surface potential ΔV (') with time at constant area, for the systems of 10 mg.L^{-1} CA + differing concentrations of HRP. Curves 1 and 1': Γ_E = 0.2 mg.m^{-2}, curves 2 and 2': Γ_E = 0.1 mg.m^{-2}

the reaction and up to the inflection point in the surface pressure kinetics. In this part of the kinetics, a 2D structure with an increasing surface concentration is the most likely organization of the interfacial layer. After the inflexion point there is a slow decrease of ΔV, which points to a reorganization process occurring in the layer. From the ellipsometric spectra taken at the end of the experiments presented in Fig. 4, the surface concentration was estimated (Table 2) to be Γ_D^* = 3.7 mg.m^{-2}. This surface concentration, as well as the decrease of ΔV and the value of ellipticity are very similar to those observed previously with surface layers of spread DHPG [9] which were assumed to form locally 3D structures (or networks) rather than a monolayer.

In conclusion, the organization of the layers formed at the initial stages of the interfacial polymerization can be tentatively referred to as 2D up to the inflection point and as 3D after it. The ΔV data in the case of the polymerization of CA (~250 mV) are higher than those obtained for monolayers of spread lignin (~150 mV) [9]. This is likely due to the presence of more free hydrophilic groups, which have a contribution to the vertical component of the dipole moment. This interpretation is consistent with previous data on the HRP induced polymerization of CA, which point to a largely dominant formation of dimers [4] at the beginning of the reaction. These dimers exhibit more free hydroxyl groups than mature DHPs, a fact which may explain the relatively higher value of ΔV with respect to DHPs.

Table 2 The change in the surface pressure and ellipticity for the interfacial layers of reaction products of the polymerization of differing quantities of HR and 10 mg.L^{-1} CA. From the ellipsometric spectrum data the thickness (h) and the refractive index (n_{layer}) of the interfacial layer were estimated using as a first approximation the Cauchy dispersion law: $n(\lambda) = A + \frac{B}{\lambda^2} + \frac{C}{\lambda^4}$, where A,B and C are constants and λ is the wavelength in nm. The surface concentration was estimated by use of Eqn. 7 (see main article text for more details)

HRP (mg.m^{-2})	Surface pressure (π)		Ellipticity ($\bar{\rho}_B$)		Estimates		
	τ_{lag} (min)	π_{max} (mN.m^{-1})	τ_{lag} (min)	$\lvert\bar{\rho}_{B(eq)}\rvert$	h (Å)	n_{layer}	Γ (mg.m^{-2})
0.1	13.0	4.8	~ 1	0.0110	39.7	1.4693	3.1
0.2	9.2	6.2	< 1	0.0143	44.1	1.4769	3.7

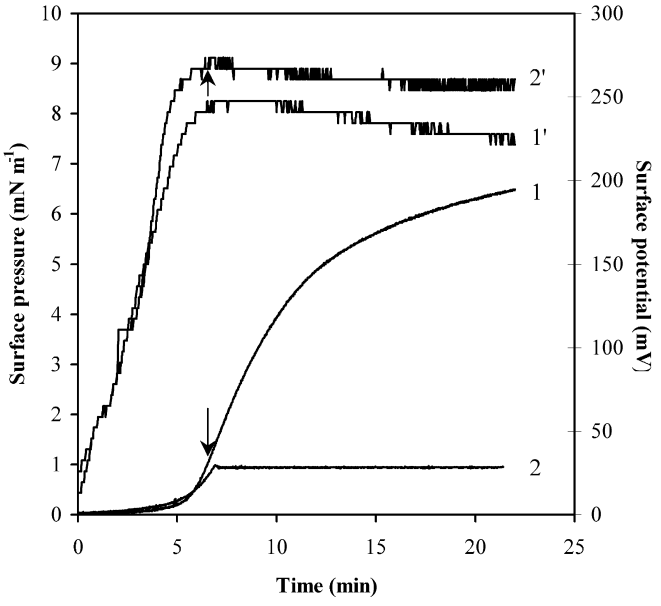

Fig. 5 Comparison between the results for the surface pressure and the surface potential ΔV (') versus time, obtained at constant area (curves 1 and 1') and at constant surface pressure (curves 2 and 2'). After the inflexion point (π_i = 1 mN.m^{-1}) ΔV (t) curves taken in the barostat regime have constant value, while for those recorded at constant area there is slow decrease. The reaction system contains 20 mg.L^{-1} CA and 0.1 mg.m^{-2} concentration of HRP. The arrows indicate where the barostat was set

In Fig. 5 the results obtained from the experiments at A = const (curves 1 and 1') and at π = const for $\pi \geq$ 1 mN/m (curves 2 and 2') for 20 mg.L^{-1} CA and 0.1 mg.m^{-2} HRP are compared. In fact, in the second option, the surface area was also constant at first and the barostat option was set at π_i = 1 mN.m^{-1}. After that point, the value of $\Delta V(t)$ was constant and a 2D monolayer structure can be assumed where the new incoming reaction products organize themselves in the available area created by the barrier movement. On the other hand, as already mentioned, at A = const a 3D structure is formed as a result of the pulling of the molecules previously at the interface by the new reaction products.

Additional evidence for the 2D-organization of the layer formed during the polymerization process can be obtained from the analysis of its reological properties.

Rheological experiments were performed after 2 hours of polymerization in a system including Γ_E = 0.2 mg.m^{-2} and C_{CA} = 6.5 mg.L^{-1}. In these conditions the surface pressure is stable and not far from the value for the surface pressure at the inflection point (π_i) where a closed packed 2D-layer is expected. Typical results are presented in Fig. 6 for $\Delta\pi(x, t)$, measured during and after compression with two different rates U_b = 180 cm^2 min^{-1} and U_b = 10 cm^2 min^{-1} (panels a, b respectively).

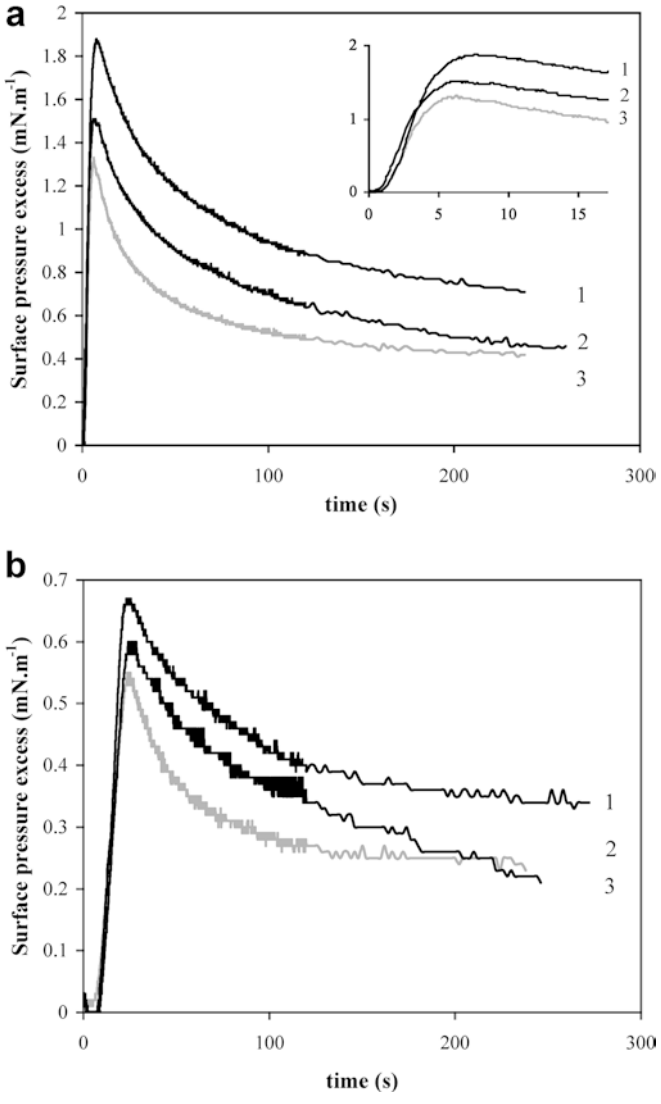

Fig. 6 Surface pressure change ($\Delta\pi$) with time (t), at various distances (x), during a compression with two different rates U_b = 180 cm^2 min^{-1} (**a**) and U_b = 10 cm^2 min^{-1} (**b**), for films formed after the polymerization of 6.5 mg.L^{-1} CA, mediated by 0.2 mg.m^{-2} enzyme. 1 - x = 20 cm, 2 - x = 30.5 cm, 3 - x = 42 cm

An elastic behavior during the compression is observed because the slope $\left(\frac{d(\Delta\pi)}{dt}\right)_x$ in the quasi-steady region does not depend on the distance x, according to Eqn. 3. A relaxation process is observed after the end of the compression and can be analyzed for $T << \tau_1, \tau_2$ by means of Eqn. 2 and data in Fig. 6a. The data obtained for E_e, E_{ne}, τ_1 and τ_2 are presented in Table 3.

These results are quantitatively similar to those obtained for 2D layers of spread DHPG (2 mg.m^{-2}) [9]. This similarity comes from the result that there are only two characteristic times of the same order of magnitude like those for DHPs [9] and that there is no third characteristic time θ ($\theta >> \tau_1, \tau_2$), responsible for the fan-like

Table 3 Characteristic times, and equilibrium (E_e) and non-equilibrium (E_{ne}) elasticity for monolayer formed after 2 hours of polymerization reaction of 6.5 mg L^{-1} CA and 0.2 mg m^{-2} HR and for monolayer built from 2 mg.m^{-2} DHPG from [9]

Material	τ_1 (s)	τ_2 (s)	E_e (mN.m^{-1})	E_{ne} (mN.m^{-1})
Products of the surface polymerization	11	70	39	30 ± 4
DHPG*	6.5	130	6	17 ± 3

dependence of $\Delta\pi(x, t)$ in the compression process as for 3D-complex layers (or network structures) [9]. From these results, it can be hypothesized that the small dimensions of the reaction products, supposed to be dimers, allow their layer to be more regular and compact than that formed by DHPG, resulting probably in the higher value of the equilibrium elasticity. In conclusion the idea of 2D organization is supported also by the analysis of the rheological analysis.

Kinetics model

In order to get an insight into the reaction mechanism of the polymerization, a kinetics model has been developed based on the results already presented and on a simplified picture of the phenomena occurring at the interface.

The reaction products are referred to as dimers; this hypothesis is reasonable at the beginning of the polymerization reaction [4]. The spread enzyme is supposed to be located at the interface. This is likely since the coverage of the interface by the enzyme is in, or close to, the gas regime (no significant surface pressure due to the protein). The reaction occurs in the sub-surface. Only the enzyme molecules and the adsorbed dimers D* are situated at the air-water interface.

The model describing the interfacial polymerization is proposed in Scheme 1.

The coniferyl alcohol (M) is brought from the bulk to the subsurface by diffusion (D is the coefficient of diffusion) and interacts with the active center of the enzyme containing Fe^{III}. The result is the formation of an enzyme-substrate complex (EM). The latter undergoes decomposition with liberation of an aroxyl radical ($^{\cdot}$M). The recombination of two radicals leads to the dimer (D) formation. It is assumed that the establishment of the steady state towards the enzyme-substrate complex and towards aroxyl radical concentration is a very fast process compared to the recombination and the adsorption of dimers at the air-water interface. It is very likely that both $^{\cdot}$M and D forms are water soluble and a part of them is taken away into the bulk phase with rate solubilization constants k_s and $k_{s'}$ respectively. A process of dimerization of two radicals in the bulk phase is also possible, but its contribution to the adsorption process of dimers at the interface is negligible because a concentration gradient is directed from the interface towards the bulk. It is assumed that there is no steady state with respect to the dimer concentration in the sub-surface. The adsorption of the dimers at the interface can be considered irreversible so that the process of desorption with rate constant k_d can be negligible with respect to the adsorption process.

In order to describe the adsorption of dimers Γ_D*(t) in a 2D-layer we shall restrict our analysis up to the inflection point of the surface pressure kinetics, corresponding to a closely packed dimer layer.

During the polymerization and the formation of the 2D-layer at constant area A_0 the rate of adsorption of dimers D* over the whole area is given by:

$$\frac{dn_{D^*}(t)}{dt} = A_0 \frac{d\Gamma_{D^*}(t)}{dt} \tag{8}$$

At constant π, this rate is expressed by:

$$\frac{dn_{D^*}(t)}{dt} = \Gamma_{D^*}^{\infty} \frac{d\Delta A(t)}{dt} \tag{9}$$

Scheme 1

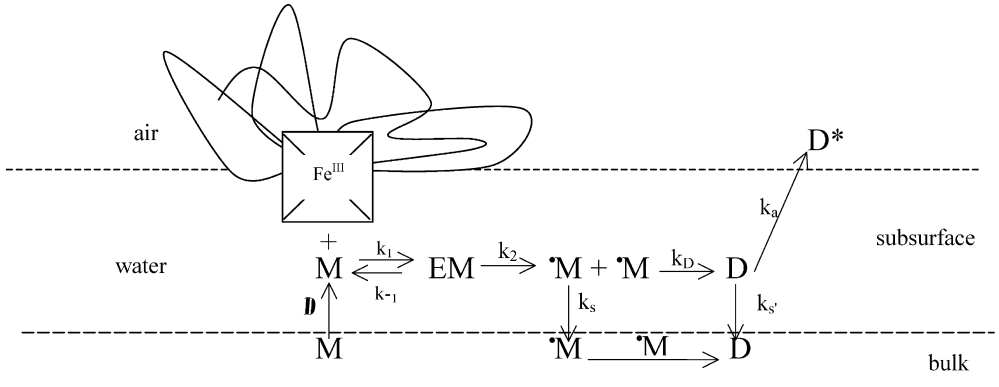

At the inflection point the two rates are equal:

$$A_0 \frac{d\Gamma_{D^*}(t)}{dt} = \Gamma_{D*}^{\infty} \frac{d\Delta A(t)}{dt} \quad (10)$$

where Γ_{D^*} [molecules cm^{-2}] is the surface concentration of dimers; Γ_{D*}^{∞} [molecules cm^{-2}] is the maximum surface concentration of dimers in the closed packed 2D-monolayer regime.

The experimental values for Γ_{D*}(t) can be obtained from ΔV experiments and Eqn.11:

$$\Gamma_{D*}(t) = \frac{\Delta V(t)}{4\pi\mu_{\perp}} \quad (11)$$

The value of $\Gamma_{D*}^{\infty}$was estimated to be 1.04×10^{14} molecules cm^{-2} in the close packed regime from a calculation of the minimum area of a dimer, using a molecular model (not shown) and calculation of $\mu_{\perp}$in this regime. If there is no change in the vertical component of the dipole moment, the evolution of Γ_D*(t) can be readily obtained from Eqn.11. The total experimental error is 15 mV ($\pm$7 mV), which corresponds to 5.58×10^{12} molecules cm^{-2}. The evolution of Γ_D*(t) can also be estimated from the ellipsometric data. As a first approximation it can be assumed that the ellipticity of the 2D-layer in the Brewster conditions for the subphase (ρ_B) is linearly proportional to Γ_D* up to the inflection point of the π(t) curve, corresponding to the maximal surface concentration $\Gamma_{D*}^{\infty} = 1.04 \times 10^{14}$ molecules cm^{-2}. With this assumption at t_i (the time corresponding to the inflection point): $\bar{p}_{Bi} \approx 1.04\times10^{14}$ molecules cm^{-2} and Γ_D*(t) = $\Gamma_{D*}^{\infty}\bar{p}_B/\bar{p}_{Bi}$.

In order to simplify the kinetics analysis, two limiting situations are considered where the limiting step is either the diffusion of substrate from the bulk or the polymerization reactions of Scheme 1. In the case where the diffusion of the substrate (coniferyl alcohol) from the bulk to the subsurface is the slower rate controlled step and the transformation of M via EM and D to D* is instantaneous by using the well-known Ward and Tordai model, without back diffusion we obtain for the rate of the dimerization process the following expression:

$$\frac{d\Gamma_{D*}}{dt} = D\left(\frac{\partial C_M}{\partial z}\right) = C_{M0}\sqrt{\frac{D}{\pi t}} \quad (12)$$

and

$$\Gamma_{D*}(t) = 2C_{M0}\sqrt{\frac{D}{\pi}}\sqrt{t} \quad (13)$$

where C_{M0} is the concentration of coniferyl alcohol (6.69×10^{16} molecules cm^{-3}, for 20 mg.L^{-1}), D is the coefficient of diffusion of CA ($D \sim 0.92\times10^{-5}$ cm^2 s^{-1} for aniline in water [22]). The substitution of these data in Eqn.13 for t = 240 s, leads to a result for Γ_D*(t) much bigger than the observed one (Γ_D* = 3.55x10^{15}molecules cm^{-2}). In other words the hypothesis of diffusion control of the polymerization is not consistent with the data because the estimated value for the diffusion coefficient ($D \sim 5\times10^{-9}$ cm^2 s^{-1}) is about 4 orders of magnitude smaller than the one extracted from the literature.

In the other limiting case the rate limiting process is the reaction of dimerization and the adsorption of the dimers, while the diffusion maintains constant the concentration C_{M0} of coniferyl alcohol in the subsurface. The following kinetic equations describe the process up to the inflection point:

$$\frac{dC_{EM}}{dt} = k_1\Gamma_E C_M - (k_{-1}+k_2)C_{EM} \quad (14)$$

$$\frac{dC_{\bullet M}}{dt} = k_2 C_{EM} - k_s C_{\bullet M} - k_D C_{\bullet M}^2 \quad (15)$$

$$\frac{dC_D}{dt} = k_D C_{\bullet M}^2 - k_s C_D - k_a C_D\left(1 - \frac{\Gamma_{D*}}{\Gamma_{D*}^{\infty}}\right) \quad (16)$$

$$\frac{1}{\delta}\frac{d\Gamma_{D*}}{dt} = k_a C_D\left(1 - \frac{\Gamma_{D*}}{\Gamma_{D*}^{\infty}}\right) \quad (17)$$

where Γ_E is the surface concentration of the enzyme [molecules cm^{-2}]; C_M [molecules cm^{-3}] is the bulk concentration of CA; C_{EM} [molecules cm^{-3}] is the concentration of enzyme-substrate complex; $C_{\cdot M}$ is the bulk concentration of the aroxyl radicals; C_D [molecules cm^{-3}] is the concentration of the dimers in the subsurface; Γ_{D^*} [molecules cm^{-2}] is the surface concentration of dimers, Γ_{D*}^{∞}[molecules cm^{-2}] is the maximal surface concentration of dimers at the air-water interface in the purely 2D regime. k_1 [cm^2 molec^{-1} s^{-1}] is the rate constant of formation of the enzyme-substrate complex; it includes δ [cm], which is the thickness of the surface phase; k_{-1} [s^{-1}] is the rate constant for the reverse process; k_2 [s^{-1}] is the rate constant for the process of formation of radicals, $k_{s'}$ [s^{-1}] is the rate constant of solubilization of the radicals, k_D [cm^3 molec^{-1} s^{-1}] is the rate constant of dimerization; k [$_{s'}$] is the rate constant of solubilization of the dimers; k_a [s^{-1}] is the rate constant of adsorption. To be consistent with the fact that the reaction is organized in the water subsurface, all concentrations must be expressed into bulk ones. The concentration of the spread enzyme and of the adsorbed dimers can be converted into bulk ones using the following definitions:

$$C_E = \frac{\Gamma_E}{\delta} \text{ and } \frac{1}{\delta}\frac{d\Gamma_{D*}}{dt} = \frac{dC_{D*}}{dt}$$

where δ [cm] is the thickness of the surface phase, C_E and C_{D^*} [molecules cm^{-3}] are the bulk concentrations of HRP and of the adsorbed dimers, respectively.

Solving this system of differential equations in the approximation of the established steady state conditions with respect to C_{EM} and $C_{\cdot M}$ leads to the following expressions for $C_{\cdot M}$, C_D (t) and Γ_{D^*} (t), respectively:

$$C_{\bullet M} = \frac{-k_s + \sqrt{k_s^2 + 4k_D \frac{k_2}{K_M} C_M \Gamma_E}}{2k_D} \tag{18}$$

where $\frac{1}{K_M} = \frac{k_1}{k_{-1}+k_2}$.

Fig. 7 The fit for the experimental data for 20 mg.L^{-1} CA and Γ_E = 0.2 mg.m^{-2} or Γ_E = 0.1 mg.m^{-2} HRP by use of the fit parameters: $k_D C_{\bullet M}^2$, k_a, $k_{s'}$. **a**: fit on ΔV experimental data, $(k_D C_{\bullet M}^2)_{0.2} \sim 13\times10^{19}$ molecules cm^{-3} s^{-1} and $(k_D C_{\bullet M}^2)_{0.1} \sim 8.5\times10^{19}$ molecules cm^{-3} s^{-1}, $k_a = 1\times10^{-3}$ s^{-1} and $k_{s'} = 1\times10^{-4}$ s^{-1}. **b**: fit on the ellipsometric data, $(k_D C_{\bullet M}^2)_{0.2} \sim 9\times10^{19}$ molec.cm^{-3}.s^{-1} and $(k_D C_{\bullet M}^2)_{0.1} \sim 6\times10^{19}$ molecules cm^{-3} s^{-1}, $k_a = 0.9\times10^{-4}$ s^{-1}, $k_{s'} = 1\times10^{-4}$ s^{-1}. The ratio between $(k_D C_{\bullet M}^2)_{0.2}$ and $(k_D C_{\bullet M}^2)_{0.1}$ is around 1.5

Since the concentration cannot be negative in Eqn.18, the plus has to be taken in front of the square root.

$$C_D(t) = \frac{k_D C_{\bullet M}^2}{\exp\left(k_s t + \int_0^t k_a \left(1 - \frac{\Gamma_{D^*}(t)}{\Gamma_{D^*}^\infty}\right) dt\right)} \times \int_0^t \exp\left(k_s t + \int_0^t k_a \left(1 - \frac{\Gamma_{D^*}(t)}{\Gamma_{D^*}^\infty}\right) dt\right) dt \tag{19}$$

$$\Gamma_{D^*}(t) = \int_0^t k_a \delta C_D(t) \left(1 - \frac{\Gamma_{D^*}(t)}{\Gamma_{D^*}^\infty}\right) dt \tag{20}$$

From Equations 19 and 20 the following expressions, valid for different periods of time, can be found:

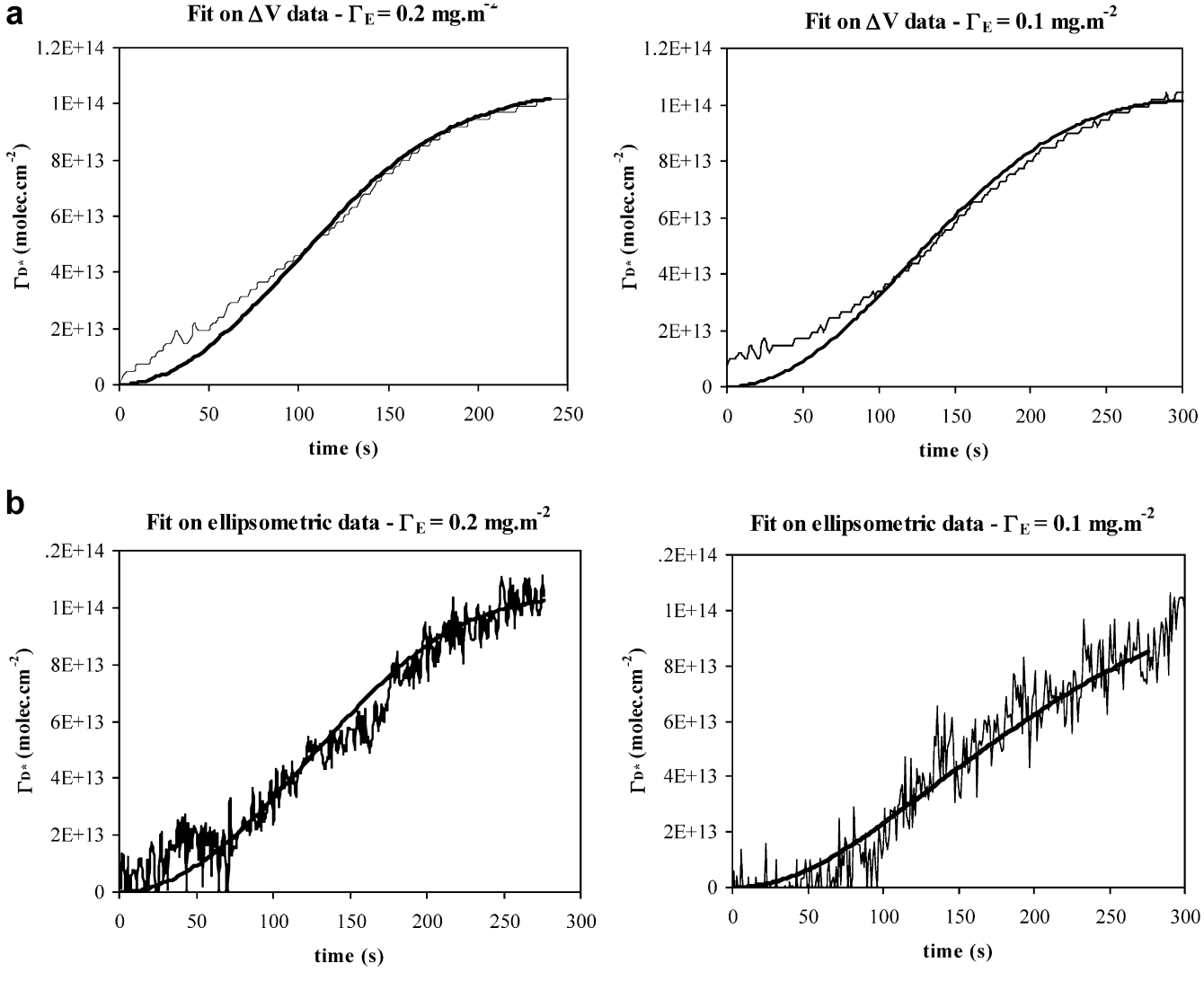

1. For $t = 0$, $C_D = 0$ and $\Gamma_{D^*} = 0$.

2. For small $t \to 0$, $\left(1 - \frac{\Gamma_{D*}(t)}{\Gamma_{D*}^{\infty}}\right) \to 1$ and $\int_0^t k_a \left(1 - \frac{\Gamma_{D*}(t)}{\Gamma_{D*}^{\infty}}\right) dt = k_a t$ and:

$$C_D(t) = \frac{k_D C_{\bullet M}^2}{(k_s + k_a)} (1 - \exp(-(k_s + k_a)t))$$

and after development in series we get

$$C_D(t) = k_D C_{\bullet M}^2 t \tag{21}$$

with

$$\Gamma_{D*}(t) = \delta \frac{k_a k_D C_{\bullet M}^2}{2} t^2 \tag{22}$$

3. For $t \to \infty$, $\Gamma_{D*}(t) \to \Gamma_{D*}^{\infty}$, $\left(1 - \frac{\Gamma_{D*}(t)}{\Gamma_{D*}^{\infty}}\right) \to 0$ and $\int_0^t k_a \left(1 - \frac{\Gamma_{D*}(t)}{\Gamma_{D*}^{\infty}}\right) dt = 0$ so

$$C_D(t) = \frac{k_D C_{\bullet M}^2}{k_s} (1 - \exp(-k_s t))$$

or in other words the concentration of dimers reaches a constant steady state value:

$$C_D = \frac{k_D C_{\bullet M}^2}{k_s} \tag{23}$$

where

$$C_{\bullet M}^2 = \frac{k_s^2 - k_s \sqrt{k_s^2 + 4k_D \frac{k_2}{K_M} C_M \Gamma_E} + 2k_D \frac{k_2}{K_M} C_M \Gamma_E}{2k_D^2} \tag{24}$$

It is obvious that the value of $C_{\bullet M}^2$ depends on the enzyme concentration Γ_E. A minimal value of the ratio $\left(C_{\bullet M}^2\right)_{\Gamma_{E1}} \Big/ \left(C_{\bullet M}^2\right)_{\Gamma_{E2}}$ for two different enzyme concentrations Γ_{E1} and Γ_{E2}, is equal to the ratio between the two concentrations Γ_{E1}/Γ_{E2} when $k_s^2 < 4k_D \frac{k_2}{K_M} C_M \Gamma_E$ or is larger when $k_s^2 \geqslant 4k_D \frac{k_2}{K_M} C_M \Gamma_E$. The system formed by Equations 19 and 20 can be numerically solved by using a minimization procedure with 3 parameters: $k_D C_{\bullet M}^2$, k_s, and k_a respectively and the previously calculated values for $\Gamma_{D*}(t)$ from ΔV data or from the ellipsometric data.

In Fig. 7 typical results are presented for the fit procedure on the ΔV and the ellipsometric data (panels a and b respectively), for the systems containing 20 mg L^{-1} CA and 0.2 or 0.1 mg m^{-2} HRP. The mean calculation error per point is 4.89×10^{12} molecules cm^{-2}, in other words within the experimental one.

The very good fit between the theoretical model and the experimental data is probably in favor of the mechanism of Scheme 1.

From the minimization procedure on the ΔV data, the following parameters were found: $k_a \sim 1 \times 10^{-3}$ s^{-1} and $k_s \sim 1 \times 10^{-4}$ s^{-1} for both systems since there was a difference in $k_D C_{\bullet M}^2$ (for 0.2 mg m^{-2} HRP average $\left(k_D C_{\bullet M}^2\right)_{0.2} \sim 13 \times 10^{19}$ molecules cm^{-3} s^{-1} and for 0.1 mg.m^{-2} HRP the average is $\left(k_D C_{\bullet M}^2\right)_{0.1} \sim 8.5 \times 10^{19}$ molecules $cm^{-3}s^{-1}$). The fit parameters obtained from the minimization procedure on the ellipsometric data are $\left(k_D C_{\bullet M}^2\right)_{0.2} = 9 \times 10^{19}$ molecules $cm^{-3}s^{-1}$, $\left(k_D C_{\bullet M}^2\right)_{0.1} = 6 \times 10^{19}$ molecules $cm^{-3}s^{-1}$, $k_a \sim 0.9 \times 10^{-3}$ s^{-1}, $k_s \sim 1 \times 10^{-4}$ s^{-1}.

It is obvious that k_a and k_s keep their constant character. The ratio between $\left(k_D C_{\bullet M}^2\right)_{0.2}$ and $\left(k_D C_{\bullet M}^2\right)_{0.1}$ is 1.53, not too far from the minimal value equal to 2. It is possible from this ratio to estimate the value of the other constants. Using the experimental values for C_M (6.692×10^{16} molecules cm^{-3}), Γ_{E1} (2.8×10^{11} molecules cm^{-2}), Γ_{E2} (1.4×10^{11} molecules cm^{-2}) and the reasonable value of 2×10^{-4} s^{-1} for k_s (roughly the solubilization of radicals is twice as fast compared to that of the dimers), from the ratio $\left(C_{\bullet M}^2\right)_{\Gamma_{E1}} \Big/ \left(C_{\bullet M}^2\right)_{\Gamma_{E2}} = 1.53$ one can obtain a value for the kinetic constant $k_D \frac{k_2}{K_M} > 2.7 \times 10^{-37} cm^5$ $molecules^{-2}$ s^{-2}. This seems reasonable, because if

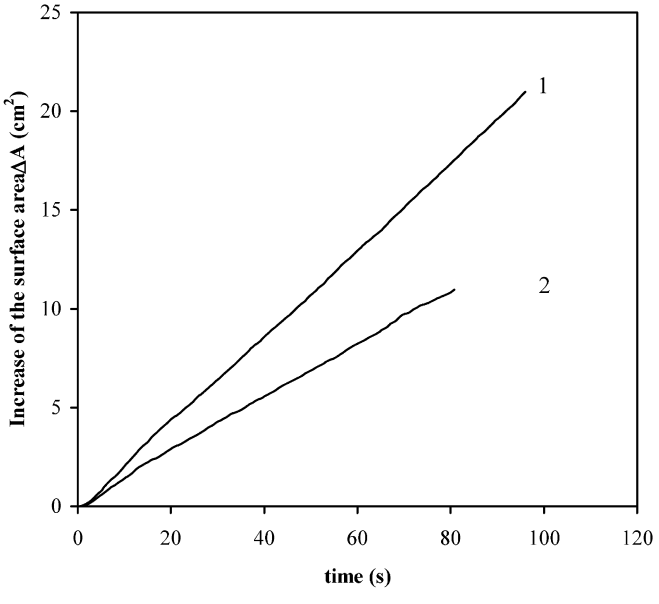

Fig. 8 The increase of the surface area ΔA with time in the case of polymerization of 20 mg.L^{-1} CA at barostat conditions (π_i = 1 mN.m^{-1}). 1 – Γ_E = 0.2 mg.m^{-2} HRP, $\left(\frac{d(\Delta A)}{dt}\right)$ = 0.2163 cm^2 s^{-1}; 2 – Γ_E = 0.1 mg.m^{-2} HRP $\left(\frac{d(\Delta A)}{dt}\right)$ = 0.1377 cm^2 s^{-1}. The ratio between the slopes is again approximately 1.5

$k_s^2 > 4k_D \frac{k_2}{K_M} C_M \Gamma_E$ then the formed radicals should be taken away into the bulk phase and no change in the surface pressure or in the ellipticity could be seen.

In Fig. 8 the increase of the surface area ΔA with time is presented for the polymerization reaction in barostratic conditions of 20 mg.L^{-1} CA with 0.2 mg.m^{-2} HRP as well as with 0.1 mg.m^{-2} HRP. The initial slope $\left(\frac{d(\Delta A)}{dt}\right)$ gives the rate of increase of the surface area. The ratio between the slopes for the different concentrations of enzyme is 1.57, again not too far from 2. This value can be interpreted considering the surface concentration of dimers in the steady state from Eqn. 23. The ratio between the rates in the case of 0.2 mg.m^{-2} and 0.1 mg.m^{-2} , Equations 17 and 21, will be again $\frac{(C^2_{\bullet M})_{0.2}}{(C^2_{\bullet M})_{0.1}}$ as discussed previously. Indeed this fact is consistent with the assumption that the rates of the polymerization process at constant π at the inflexion point and at constant A are equal. Moreover, the value of the slope in Fig. 8 can be calculated, since from Eqn. 10 we have:

$$\frac{d(\Delta A)}{dt} = \frac{d\Gamma_{D*}(t)}{dt}\frac{A_0}{\Gamma_{D*}}$$

from Eqn. 17 so we can estimate the value for $\frac{d\Gamma_{D*}(t)}{dt}$. For the example of 0.1 mg.m^{-2} HRP and 20 mg.L^{-1}, near the inflection point, from the minimization procedure we have $k_s = 1\times10^{-3}$ s^{-1}; $\delta = 1\times10^{-7}$ cm; $\left(1 - \frac{\Gamma_{D*}(t)}{\Gamma^{\infty}_{D*}}\right) =$ 0.0697 and for $C_D = 2.4\times10^{22}$ molecules cm^{-3}, and for the theoretical slope a value of 0.137 is obtained, as compared to the experimental value of 0.138 cm^2 sec^{-1} (see Fig. 8).

Conclusions

In conclusion, the initial stage of the enzyme mediated polymerization reaction of coniferyl alcohol, taking part at the air-water interface, was studied. The rate of the reaction depends on the concentration of both the coniferyl alcohol and the enzyme. The process is probably organized in the subsurface. In constant area conditions the reaction leads to the formation of a complex, probably 3D layer, while in constant low surface pressure conditions the organization seems to be a quasi-monolayer. The proposed kinetic model assumes that the evolution of the monitored surface properties (surface pressure, surface potential and ellipticity) is due to the adsorption of dimers, which are the reaction products in the initial phase of the polymerization. The rate-limiting step is the adsorption of the products, not the diffusion of the substrate molecules.

Acknowledgements Our warm thanks extend to B. Monties for his interest in the present work. The program Cocop from Ministère des Affaires Etrangères DSUR-NGE-4C1–701 financially supported this work.

References

1. Adler E (1997) Wood Sci Technol 11:169
2. Nimz H (1974) Angew Chem, Int Ed 13:313
3. Karhunen P, Sipilä J, Rummahko P, Brunow G (1995) Tetrahedron Lett 36:169
4. Sarkanen KV (1971) In: Sarkanen KV, Ludwig GH (eds) Lignins: Occurrence, formation, structure and reactions. Wiley, New York, p95
5. Cathala B, Saake B, Faix O, Monties B (1998) Polym Degrad Stab 59:65
6. Baumberger S, Aguié-Béghin V, Douillard R, Lapierre C, Monties B (1997) Ind Crops Products 6:259
7. Cathala B, Lee LT, Aguié-Béghin V, Douillard R, Monties B (2000) Langmuir 16:10444
8. Luner P, Kempf U (1970) Tappi J 53:2069
9. Grozev N, Aguié-Béghin V, Ivanova Tz, Baumberger S, Cathala B, Douillard R, Panaiotov I (2002) Colloid Polym Sci 280:798
10. Bruno FF, Akkara JA, Kaplan DL, Sekher P, Marx KA, Tripathy SK (1995) Ind Eng Chem Res 34:4009
11. Bruno FF, Akkara JA, Samuelson LA, Kaplan DL, Mandal BK, Marx KA, Kumar J, Tripathy SK (1995) Langmuir 11:889
12. Rubner MF, Hong K (1988) Thin Solid Films 160:187
13. Cathala B, Aguié-Béghin V, Douillard R, Monties B (2002) In: Renard G. Della Valle, Popineau Y (eds) Plant biopolymer science: Food and non food applications. Royal Society of Chemistry, Cambridge, p. 173
14. Ludley FH, Ralph J (1996) J Agric Food Chem 44:2942
15. Trurnit HJ (1960) J Colloid Sci 15:1
16. Panaiotov I (2000) Ann Univ Sofia, Fac Chim 88: 121
17. Panaiotov I, Dimitrov DS, Ter-Minassian Saraga L (1979) J Colloid Interface Sci 72:49
18. Dimitrov DS, Panaiotov I (1980) In: Georgiev G (ed) Prog. II Symposium "Lung lipid metabolism...", Varna, May 19–24, 1979. Publishing House of the Bulgarian Academy of Sciences, Sofia
19. Manning-Benson S, Bain CD, Darton RC (1997) J Colloid Interface Sci 189:109
20. De Feijter JA, Benjamins J, Veer FA (1978) Biopolymers 17:1759
21. Aguié-Béghin V, Baumberger S, Monties B, Douillard R (2002) Langmuir 18:5190
22. Lide DR (ed) (1990) Handbook of Chemistry and Physics, 70th edn. CRC, Boca Raton, Florida